

## Article

# Design and Experimental Research on a Chisel-Type Variable Hierarchical Deep Fertilization Device Suitable for Saline–Alkali Soil

Nan Xu <sup>1,2</sup>, Zhenbo Xin <sup>1,3</sup>, Jin Yuan <sup>1,3</sup> , Zenghui Gao <sup>2</sup>, Yu Tian <sup>2</sup>, Chao Xia <sup>2</sup>, Xuemei Liu <sup>1,3,\*</sup>   
and Dongwei Wang <sup>2,\*</sup>

<sup>1</sup> College of Mechanical & Electronic Engineering, Shandong Agricultural University, Tai'an 271018, China; 2021010105@sdau.edu.cn (N.X.); xinzb@sdau.edu.cn (Z.X.); jyuan@sdau.edu.cn (J.Y.)

<sup>2</sup> Yellow River Delta Intelligent Agricultural Machinery and Equipment Industry Research Academy, Dongying 257345, China; gaoqau@163.com (Z.G.); yrdia@yrdia.cn (Y.T.); xia102002@163.com (C.X.)

<sup>3</sup> Shandong Agricultural Equipment Intelligent Engineering Laboratory, Tai'an 271018, China

\* Correspondence: lxmywj@126.com (X.L.); w88030661@163.com (D.W.); Tel.: +86-152-6986-8559 (X.L.)

**Abstract:** In China, there are around 36.7 million hectares of saline–alkali lands that hold utilization potential. Precision fertilization stands as a vital measure for enhancing the quality of saline–alkali soil and promoting a significant increase in crop yields. The performance of the fertilization device is a decisive factor in determining the effectiveness of fertilization. To optimize the fertilizer utilization rate in coastal saline–alkali soils and substantially reduce fertilizer waste, it is imperative to transport fertilizers to the deep soil layers and execute layered variable-rate fertilization. In light of this, a chisel-type variable-rate layered electronically controlled deep-fertilization device specifically designed for saline–alkali soils has been developed. Extensive experimental research on its fertilization performance has also been carried out. Drawing on the principles of soil dynamics, this paper meticulously investigates the structures of key components and the operating parameters of the fertilization device. Key parameters such as the penetration angle of the fertilizer shovel, the penetration clearance angle, the curvature of the shovel handle, the angle between the fertilizer baffle and the fertilizer pipe wall, the angle between the fertilizer pipe and the horizontal plane, and the forward speed are precisely determined. Moreover, this study explores the quantitative relationship between the fertilizer discharge amount of the fertilizer applicator and the effective working width. Simultaneously, this research mainly focuses on analyzing the impact of the forward speed on the operational effect of layered and variable-rate fertilization. Through a series of field experiments, it was conclusively determined that the optimal fertilization effect was attained when the forward speed was set at 6 km/h. Under this condition, the average deviation in the fertilization amount was merely 2.76%, and the average coefficients of variation in the fertilizer amount uniformity in each soil layer were 7.62, 6.32, 6.06, and 5.65%, respectively. Evidently, the experimental results not only successfully met the pre-set objectives, but also fully satisfied the design requirements. Undoubtedly, this article can offer valuable methodological references for the research and development of fertilization devices tailored for diverse crops cultivated on saline–alkali lands.



Academic Editor: Caiyun Lu

Received: 3 January 2025

Revised: 15 January 2025

Accepted: 17 January 2025

Published: 18 January 2025

**Citation:** Xu, N.; Xin, Z.; Yuan, J.; Gao, Z.; Tian, Y.; Xia, C.; Liu, X.; Wang, D. Design and Experimental Research on a Chisel-Type Variable Hierarchical Deep Fertilization Device Suitable for Saline–Alkali Soil. *Agriculture* **2025**, *15*, 209. <https://doi.org/10.3390/agriculture15020209>

**Copyright:** © 2025 by the authors. Licensee MDPI, Basel, Switzerland. This article is an open access article distributed under the terms and conditions of the Creative Commons Attribution (CC BY) license (<https://creativecommons.org/licenses/by/4.0/>).

**Keywords:** saline–alkali land; layered fertilization; variable rate fertilization; soil dynamics

## 1. Introduction

Soil is the most fundamental and crucial production resource in agriculture. According to the 'Main Data Bulletin of the Third National Land Survey', China's cultivated land area is 128 million hectares [1], ranking third in the world, only after the United States and India. However, the per capita arable land area is merely 0.0933 hectares, ranking 126th globally. The per capita cultivated land area of Canada is 18 times that of China, indicating an acute shortage of arable land resources in China. Additionally, China has approximately 36.77 million hectares of saline–alkali land that can be utilized. Reasonably developing and utilizing saline–alkali land for crop cultivation is one of the important ways to relieve the shortage of arable land resources in the country [2,3]. Moreover, precision fertilization is one of the key means to improve soil quality and characteristics, thereby increasing crop yields [4].

At present, deep fertilization [5,6], layered fertilization [7,8], and variable-rate fertilization [9] have become fertilization methods that can promote crop absorption and utilization and improve fertilizer efficiency [10,11], enabling crop yield increase [12], fertilizer reduction [13], and sustainable soil use [14]. Fertilization quality is one of the factors affecting crop yields, and the fertilization device determines the fertilization effect [15,16]. In recent years, researchers have carried out designs and relevant studies on deep-fertilization [17,18], layered fertilization [19–21], and variable-rate fertilization devices [22–25]. In 2020, Liao Yitao et al. [26] designed an active anti-blocking deep-fertilization device suitable for direct seeding of rapeseed in the rice–rape rotation area. They used the discrete element method to analyze the influence of key structural parameters of the fertilizer shovel on the movement state of fertilizer particles, effectively achieving deep fertilization for rapeseed. Yang Qinglu et al. [27] designed a spatial layered fertilization device for corn, which can accurately achieve layered fertilization and adjust the fertilization ratio of each layer according to agronomic requirements, facilitating corn growth. In 2021, Han Lianjie et al. [28] designed an electronically controlled fertilizer discharging device based on the PID algorithm, which can achieve variable-rate fertilization and improve the uniformity and accuracy of fertilization. Zhao Yanzhong et al. [29] designed a side-deep layered fertilization component for no-tillage seeding machines, reducing the number of times of top-dressing machinery entering the field and improving fertilizer utilization efficiency.

To improve the fertilizer utilization rate of coastal saline–alkali soil and reduce fertilizer waste, it is necessary to deliver fertilizers to the deep soil layer and carry out layered variable-rate fertilization. However, the surface layer of coastal saline–alkali soil is severely compacted, and the deep layer is heavy clay soil, resulting in a relatively complex working condition. When deep-fertilization devices operate in coastal saline–alkali soil, problems such as high resistance and large-scale rigid soil disturbance may occur. During the operation of existing layered fertilization devices, issues such as back-filling saline–alkali soil particles and numerous collisions between fertilizer particles, which lead to mixed fertilization, prevent the achievement of an effective layered fertilization effect [30,31]. At the same time, to achieve effective layered fertilization operations and complete a reasonable ratio of fertilizer application amounts in the upper and lower layers of deep-fertilization, a variable-rate fertilization device is required to control the fertilizer discharge amount [32]. Based on the characteristics of coastal saline–alkali soil, taking the fertilization for cotton production, which is suitable for growing in saline–alkali land, as an example, a chisel-type variable-rate and layered deep-fertilization device suitable for saline–alkali soil was designed. The structural parameters of key fertilization devices such as the fertilization shovel were determined by means of the in-depth integration of agricultural machinery and agronomy and the application of soil dynamics. Moreover, a combination of discrete

element virtual tests and field tests was adopted to conduct performance test research on layered and variable-rate fertilization for motion parameters.

## 2. Materials and Methods

The quality of fertilization exerts a profound influence on crop yields. Taking fertilization in cotton production as an illustrative case, in line with the agronomic stipulations put forward in the ‘Opinions on Cotton Pre-sowing and Sowing Techniques in Shandong Province in 2023’, for short-season cotton, all of the chemical fertilizers needed throughout its growth cycle must be deeply applied in one go into the saline–alkali soil at a depth of below 120 mm. In response to this requirement, a chisel-type variable-rate layered deep-fertilization device, which is well-adapted to saline–alkali soil conditions, has been meticulously designed.

### 2.1. Determination of Physical Properties of Saline–Alkali Soil

The designed chisel-type deep-fertilization device mainly consists of a fixed frame, a deep-loosening furrow opener, fertilizer guide pipes, reinforcing ribs, fertilizer tubes, etc. The structure is shown in Figure 1. In order to achieve a fertilization depth of 120 mm and ensure effective soil back-filling after furrowing, a chisel-type deep-loosening fertilizer shovel was designed as the furrowing device. Key parameters of the chisel-type deep-loosening shovel were studied to increase the disturbance coefficient of saline–alkali soil, improve the fertilizer utilization effect, increase the back-filling rate of saline–alkali soil, ensure the fertilization depth, and avoid the formation of deep ditches that could lead to waterlogging. The soil is disturbed by the action of the shovel tip and the shovel body, forming a fertilizer furrow with an adjustable depth of 120–150 mm. The fertilizer particles flowing into the shovel fall into the fertilizer furrow in the form of strip-shaped layered application. The saline–alkali soil back-fills the furrow under its own gravity, burying the fertilizer particles.

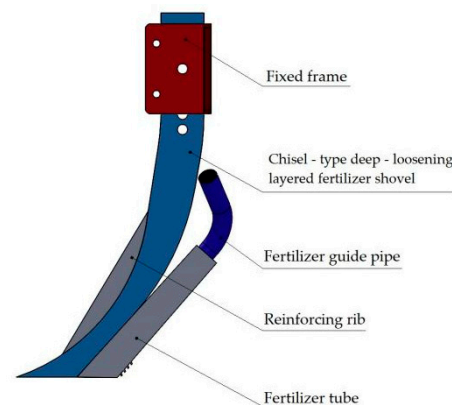


**Figure 1.** Chisel-type deep-loosening fertilization device with adjustable depth.

### 2.2. Structural Design of Chisel-Type Deep-Loosening Layered Fertilizer Shovel

Due to the relatively deep fertilization depth, the fertilizer shovel has to bear significant resistance. Meanwhile, considering the special nature of the saline–alkali soil, which is severely compacted and heavy-textured, in order to reduce the resistance, decrease the contact area with the soil, and minimize the rigid disturbance to the soil, a chisel-type deep-loosening shovel is selected as the fertilization and furrowing mechanism. Design and performance improvement work is carried out based on the existing structure of the chisel-type deep-loosening shovel to meet the requirements of high-quality fertilization operations for cotton.

Based on the structure and composition of the chisel-type deep-loosening layered fertilizer shovel, through the force analysis of each component, it can be seen that the main force-bearing components are the shovel handle and the shovel tip. The shovel handle is subject to relatively large resistance. While ensuring its strength, the structure of the shovel handle should be optimized to reduce the operating resistance. The shovel tip, as the core component affecting the deep-loosening and fertilization effects, in order to reduce the penetration resistance and, at the same time, prepare a high-quality landing area for granular fertilizers to improve the fertilization quality, requires optimization design and performance improvement of its structure and installation position.

### 2.2.1. Structural Design and Performance Optimization of the Shovel Tip Based on Dynamics

A rectangular coordinate system is established with the shovel tip as the origin, and the forces acting on the shovel tip are analyzed, as shown in Figure 2.

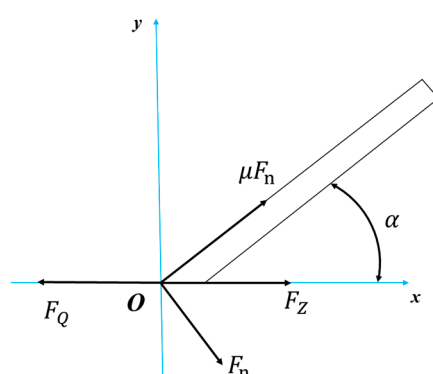


**Figure 2.** Force analysis of the shovel tip.

To reduce the soil resistance of the shovel tip, a mathematical model of the force on the shovel tip, with respect to soil resistance, needs to be established. According to the force analysis of the shovel tip in the horizontal direction, it can be obtained that

$$F_Z = F_Q - \mu F_n \cos \alpha - F_n \sin \alpha \quad (1)$$

In the formula, the symbols represent the following:

- $F_Z$ —The resistance of the soil to the shovel tip, N;
- $F_Q$ —The traction force in the horizontal direction, N;
- $\mu$ —The coefficient of sliding friction between the shovel tip and the soil;
- $F_n$ —The normal load of the soil on the shovel tip, N;
- $\alpha$ —Penetration angle, °.

From the model, it is evident that the primary factors influencing the magnitude of soil resistance encompass the sliding friction coefficient between the shovel tip and the soil, the normal load exerted by the soil on the shovel tip, and the penetration angle. Notably, when the material of the shovel tip remains unaltered, the sliding friction coefficient stays constant. Consequently, the emphasis lies on the impacts of the soil's normal load on the shovel tip and the penetration angle on the magnitude of soil resistance.

Consequently, it is necessary to analyze the forces acting on the soil mass on the inclined surface of the shovel tip. A rectangular coordinate system is established with the shovel tip as the origin, and the weight of the soil mass is  $mg$ , as shown in Figure 3.

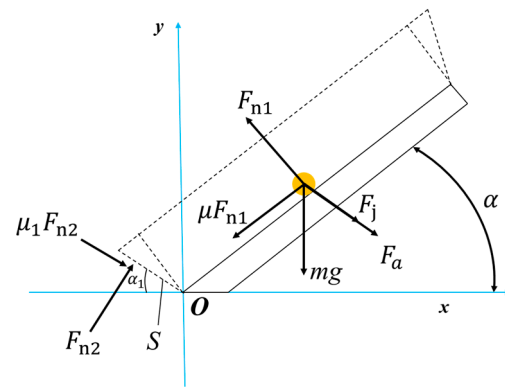


Figure 3. Force analysis of the soil.

Establish the force–balance equations of the soil in the horizontal and vertical directions, respectively.

$$\begin{cases} F_{n1}(\sin\alpha + \mu\cos\alpha) - (F_jS + F_a)\cos\alpha_1 = F_{n2}(\sin\alpha_1 + \mu_1\cos\alpha_1) \\ mg - F_{n1}(\cos\alpha - \mu\cos\alpha) + (F_jS + F_a)\sin\alpha_1 = F_{n2}(\cos\alpha_1 - \mu_1\cos\alpha_1) \end{cases} \quad (2)$$

In the formula, the symbols represent the following:

- $F_{n1}$ —The normal load exerted by the inclined surface of the shovel tip on the soil, N;
- $F_j$ —Soil cohesion, N;
- $S$ —Failure area of the shear plane,  $\text{mm}^2$ ;
- $F_a$ —Soil accelerating force, N;
- $F_{n2}$ —The normal load on the failure surface of the soil, N;
- $\alpha_1$ —The angle between the soil failure surface and the horizontal direction,  $^\circ$ ;
- $\mu_1$ —Coefficient of friction between soils.

During the operation of the fertilization shovel, the traction force is equal in magnitude and opposite in direction to the soil resistance received by the shovel tip. By simultaneously solving with the above equation, the force mathematical model of the soil resistance is obtained:

$$f = \frac{\left( mg + \frac{F_jS + F_a}{\sin\alpha_1 + \mu_1\cos\alpha_1} \right)}{\left( \frac{\cos\alpha_1 - \mu_1\sin\alpha_1}{\sin\alpha + \mu\cos\alpha} + \frac{\cos\alpha_1 - \mu_1\sin\alpha_1}{\sin\alpha_1 + \mu_1\cos\alpha_1} \right)} \quad (3)$$

In the formula,  $f$ —soil resistance.

To simplify the model, let

$$\frac{\cos\alpha_1 - \mu_1\sin\alpha_1}{\sin\alpha + \mu\cos\alpha} + \frac{\cos\alpha_1 - \mu_1\sin\alpha_1}{\sin\alpha_1 + \mu_1\cos\alpha_1} = i \quad (4)$$

Then, the above formula can be obtained as follows:

$$f = \frac{mg}{i} + \frac{F_jS + F_a}{i(\sin\alpha_1 + \mu_1\cos\alpha_1)} \quad (5)$$

As can be inferred from the force-based mathematical model, soil resistance is primarily related to factors such as the penetration angle, the failure area of the shear plane, soil cohesion, soil accelerating force, and the angle between the failure plane and the horizontal direction. From the force analysis diagram, it can be seen that the failure area of the shear plane and the angle between the failure plane and the horizontal direction are related to the magnitude of the penetration angle. Moreover, soil cohesion and soil accelerating force are physical parameters inherent to the soil itself. Therefore, when the structural parameters of

the shovel tip are determined, the magnitude of soil resistance is related to the penetration angle. As the penetration angle increases, the resistance increases. However, when the penetration angle is relatively small, it is difficult to achieve effective deep soil loosening. By substituting values into the mathematical model for calculation and evaluation, and in light of the design requirements of the sub-soiling and fertilizing shovel, the penetration angle is determined to be 20°. Meanwhile, based on the design method of sub-soiler in the Agricultural Machinery Design Manual, research was carried out and the penetration clearance angle  $\alpha_2$  was determined to be 10°.

### 2.2.2. Research on the Energy-Saving and Resistance-Reducing Structural Design of the Shovel Shank

Under the premise of ensuring strength, the main way to reduce the operating resistance is through the geometric design of the shovel shank curve. According to the references [33], the equations of the shovel shank curves of various soil-contacting components mainly include logarithmic function curves, exponential function curves, and power function curves, etc. However, for sub-soiling shovels, the exponential function is mostly used for design improvement. Therefore, targeted optimization of the exponential function shovel shank curve is carried out to achieve the optimal operating effect.

A rectangular coordinate system is established with the origin O for the design analysis of the exponential function shovel shank curve. The coordinate system of the exponential function shovel shank curve is shown in Figure 4. Point A is the starting point of the shovel shank curve, with coordinates  $(x_A, y_A)$ , and point B is the ending point of the shovel shank curve and also the soil penetration point of the sub-soiling shovel, with coordinates  $(x_B, y_B)$ .

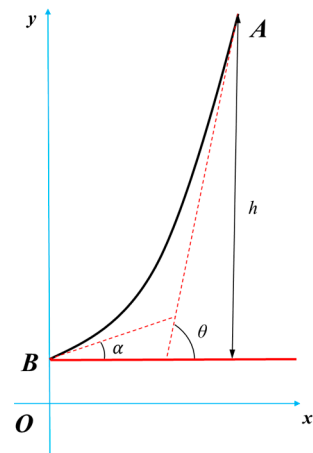


Figure 4. Exponential function shovel shank curve.

The equation of the exponential function shovel shank curve can be set as

$$y = a^x \tag{6}$$

In the formula,  $a$ —the base of the exponential function for the shovel shank curve ( $a$  is a constant and  $a > 0, a \neq 1$ ).

Derive points A and B, respectively, and express the geometric relationships based on the exponential function shovel shank curve. Then the following expressions can be obtained:

$$\begin{cases} y'_A = a^{x_A} \ln a = \tan\theta \\ y'_B = a^{x_B} \ln a = \tan\alpha \end{cases} \tag{7}$$

In the formula,  $\theta$ —the starting angle of the tangent to the exponential function shovel-shank curve, deg.

In the figure,  $h$  represents the vertical height difference between the starting point and the soil entry point of the shovel shank curve, and its quantitative relationship is

$$y_A - y_B = h \quad (8)$$

By simultaneously considering the above three equations, the mathematical relationship among the base  $a$  of the exponential function shovel shank curve, the soil penetration angle, and the starting angle of the curve's tangent is obtained.

$$a = e^{\frac{\tan\theta - \tan\alpha}{h}} \quad (9)$$

And the optimized mathematical model of the shovel shank curve is obtained.

$$y = a^x = \left( e^{\frac{\tan\theta - \tan\alpha}{h}} \right)^x \quad (10)$$

From the above formula, it can be seen that the starting angle of the tangent to the shovel shank curve, the soil penetration angle of the shovel shank, and the vertical height difference between the starting point and the soil penetration point of the shovel shank curve affect the specific shape of the shovel shank curve. According to the cotton planting agronomy described above,  $h = 150$  mm, and the starting angle  $\theta$  of the tangent to the shovel shank curve is designed to be  $75^\circ$ . Based on the above-mentioned results of the shovel tip structural design and performance optimization, the soil penetration angle of the shovel shank is  $20^\circ$ . Calculated according to the determined key structural parameters, the base  $a$  of the exponential function shovel shank curve is determined to be 1.02. Therefore, the equation of the exponential function shovel shank curve is

$$y = 1.02^x \quad (11)$$

Design the shovel shank according to the exponential function shovel shank curve.

### 2.3. Structural Design of the Fertilizer Tube

In line with the agronomic requirements of cotton cultivation, implementing a layered fertilization operation is essential. This approach not only enhances the efficacy of fertilizer application, but also concurrently cuts down on the quantity of fertilizers utilized. The fertilizer tube plays a pivotal role, as it significantly impacts both the uniformity of fertilizer distribution and the effectiveness of the layered fertilization process. Consequently, it is imperative to conduct a meticulous design of the structural parameters of the fertilizer tube to ensure optimal performance in cotton planting fertilization operations.

A fertilizer tube capable of achieving four-layer fertilization is designed, which can meet the agronomic requirement that the amount of fertilizer applied increases layer by layer from top to bottom. The structure of the fertilizer tube is shown in Figure 5. Numbers 1–4 are the four-layer fertilizer outlets, respectively. When fertilizer particles enter the fertilizer tube through the feed inlet, they fall in the fertilizer tube. After hitting the fertilizer baffles of different lengths, they are subjected to different forces and thus exhibit different motion states.

As can be seen from the figure, the main factors affecting the uniformity of fertilizer application and the effect of layered fertilization include the length  $l$  of the baffles at different fertilizer outlets, the angle between the fertilizer baffle and the wall of the fertilizer tube, the angle between the fertilizer tube and the horizontal  $x$ -axis, etc., among them, and

these affect the opening direction and position of the fertilizer outlet, while  $l$  affects the amount of fertilizer discharged from the fertilizer outlet.

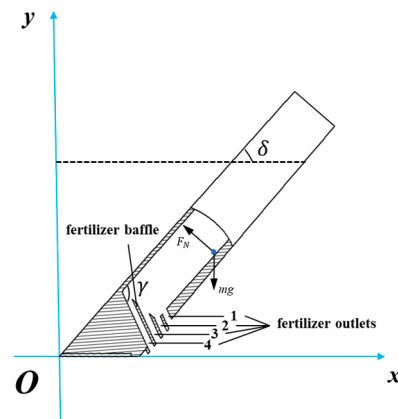


**Figure 5.** Structural parameters of the fertilizer tube and the force diagram of the fertilizer.

When the fertilizer particles come into contact with the tube wall, ignoring the rolling friction between the particles and the tube wall, the particles are acted upon by the gravitational force  $mg$  and the supporting force  $F_N$ . When the fertilizer particles just slide down along the tube wall, the force acting on the fertilizer particles is  $F_N = mgsin\delta$ ; when  $F_N > mgsin\delta$  occurs, the motion state of the fertilizer particles can be divided into two types. The first scenario is that the fertilizer particles slide down along the fertilizer baffle to complete the fertilization operation. The second is that they collide with the fertilizer baffle and then cross the baffle to enter the next fertilizer outlet area. By designing the front ends of the second and third baffles to be inclined, the direction of the force exerted on the fertilizer particles can be altered. In other words, the motion state of the fertilizer particles is changed, allowing for some of them to enter the next fertilizer outlet area after the collision. This meets the requirement that the amount of fertilizer applied increases progressively from the upper layer to the lower layer, thus optimizing the layered fertilization effect.

According to the design method of the layered fertilization structure in references [33,34], analyze the movement state of fertilizer particles at each stage by referring to it. Combine with the agronomic requirement that the amount of fertilizer applied is less in the upper part and more in the lower part for cotton fertilization, and then design the key structural parameters of the fertilizer pipe. The angle  $\gamma$  between the fertilizer baffle and the fertilizer tube wall is  $115^\circ$ , the angle  $\delta$  between the fertilizer tube and the horizontal  $x$  axis is  $50^\circ$ , and the lengths  $l$  of the baffles at different fertilizer outlets are 16 mm, 27 mm, 50 mm, and 65 mm, respectively.

#### 2.4. Design of the Variable Fertilizer-Discharging Device

##### 2.4.1. Fertilization Agronomic Requirements

The seeding- and fertilization-integrated machine is used to apply all the chemical fertilizers required for the whole growth period of cotton at one time (with a depth of  $\geq 12$  cm) during seeding. The amount of fertilizers includes 5–7 kg of pure nitrogen, 8–10 kg of phosphorus pentoxide, and 10–12 kg of potassium oxide per  $666.67 \text{ m}^2$ , totaling about 23–29 kg.

##### 2.4.2. Design of the Electric-Controlled Fertilizer-Discharging Device

An electric-controlled fertilizer discharging device is designed. The device adopts a traditional external fluted-wheel fertilizer discharger, and a motor is used to control the speed of the fertilizer discharger. The rest mainly consists of system hardware such as a motor driver, a speed-measuring radar, and an STM32 single-chip microcomputer. The basic principle of the control system is shown in Figure 6.

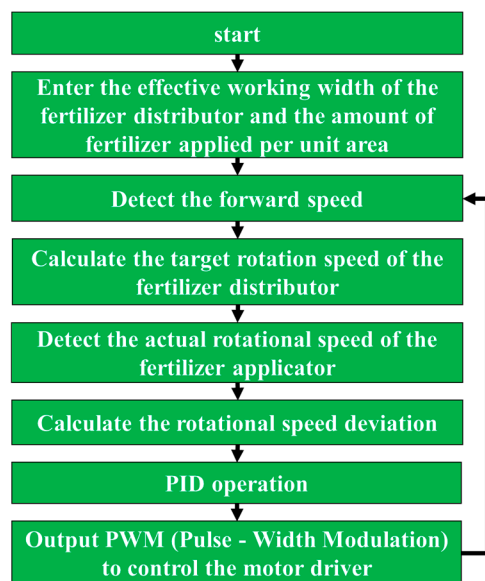


**Figure 6.** Principle of the control system.

As a result of this research, the STM32F103RCT6 (STMicroelectronics Co., Ltd., Shanghai, China) embedded micro-controller is selected as the main control chip of the electric-controlled fertilizer discharging device. Its key feature is that it can directly control the working state of the motor driver through the output of PWM signals. Its performance parameters are shown in Table 1.

**Table 1.** Performance parameters of STM32F103RCT6 embedded micro-controller.

|                         |                             |
|-------------------------|-----------------------------|
| Core bit width          | 32-bit                      |
| Maximum main frequency  | 72 MHz                      |
| Peripheral device       | DMA, Motor Control PWM etc. |
| Program memory capacity | 256 KB                      |
| RAM capacity            | 48 K                        |
| Connectivity            | CAN, UART, ADC, IIC etc.    |

After selecting the traditional external fluted-wheel fertilizer discharger as the fertilizer discharging device, the 36GX555 planetary gear (Shenzhen ZhaoWei Technology Co., Ltd., Shenzhen, China) reduction motor is chosen to provide power for the external fluted-wheel fertilizer discharger. Its performance parameters are shown in Table 2.

**Table 2.** 36GX555 planetary gear reduction moto.

|                 |           |
|-----------------|-----------|
| Nominal voltage | 12 V      |
| Rated torque    | 7 kg/cm   |
| No-load speed   | 150 r/min |
| Reduction ratio | 50        |

Based on the determination of the main control chip and the actuator motor, a motor driver using the NCE80H11 MOSFET (Wuxi NCE Power Semiconductor Co., Ltd., Wuxi, China) is selected through research. Its performance parameters are shown in Table 3.

**Table 3.** Performance parameters of the motor driver.

|                     |          |
|---------------------|----------|
| Input voltage       | 12 V     |
| Rated current       | 12 A     |
| PWM effective range | 0.1–100% |

A speed-measuring radar (Hangzhou Lailai Technology Co., Ltd., Hangzhou, China) is adopted to monitor and input the forward speed of the machine in real time. The speed-measuring radar is installed at the rear of the seeder frame. During the machine's movement, the Doppler sensor in the speed-measuring radar generates pulse signals using the Doppler principle, accurately measuring the traveling speed of the seeder in the field. Its performance parameters are shown in Table 4.

**Table 4.** Performance parameters of the speed-measuring radar.

|                            |             |
|----------------------------|-------------|
| Operating frequency        | 24 GHz      |
| Speed measurement range    | 0.5–30 km/h |
| Speed measurement accuracy | ±0.1 km/h   |

### 2.5. Influence of Forward Speed on the Effect of Fertilization Operation

Once the design of the structural parameters for the key components of the chisel-type variable-rate layered deep-fertilization device is completed, the determination of the motion parameters of the fertilization device becomes imperative. Among these motion parameters, the forward speed is a primary factor. It is essential to conduct in-depth exploration into how the forward speed impacts the layered and variable-rate fertilization operation effects of the fertilization device. This exploration aims to enhance the overall quality of the layered and variable-rate fertilization operations, ensuring that the fertilization process is more precise, efficient, and better adapted to the specific needs of different soil conditions and crop growth requirements.

#### 2.5.1. Influence of Forward Speed on the Effect of Layered Fertilization Operation

In order to thoroughly investigate the correlations among the forward speed, the fertilization amount of each layer, and the fertilization uniformity, it is necessary to conduct an experimental analysis. Nevertheless, collecting field test data poses significant challenges. Therefore, a simulation analysis grounded in the discrete element method must be adopted for research purposes. A discrete element simulation model is constructed based on the calibrated intrinsic parameters and contact parameters, which serves as a crucial tool for the in-depth exploration of these relationships.

Based on the structural design of the fertilization device described above, the three-dimensional model was drawn using Solidworks 2022 (Dassault Systèmes Co., Ltd., Waltham, MA, USA), and its structural dimensions are shown in Figure 7.

##### (1) Calibration of discrete element simulation parameters.

First, complete the parameter calibration of fertilizer particles according to the same method as for soil parameter calibration [35], conduct experimental verification, and obtain the intrinsic parameters of fertilizer particles as well as the contact parameters of fertilizer–fertilizer, fertilizer–soil, fertilizer–fertilization pipe, and soil–fertilization pipe. The results are shown in Table 5 [36].

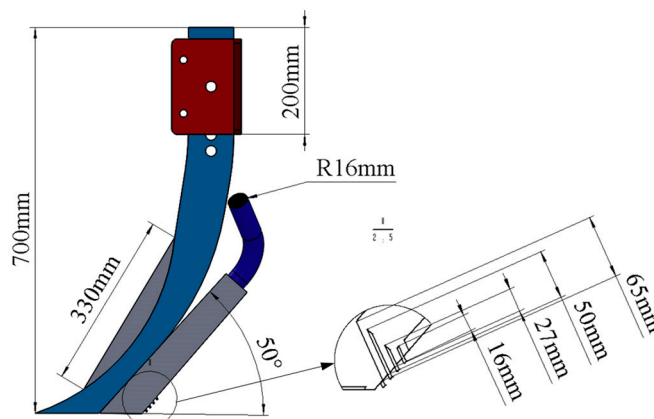
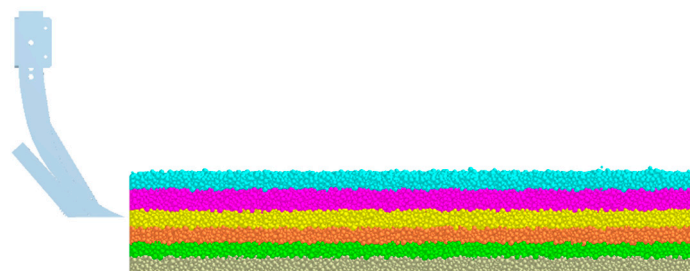


Figure 7. Key dimensional parameters of the fertilization device.

Table 5. Calibration results of discrete element simulation parameters.

| Soil Depth/cm  | 0–5             | 5–10            | 10–15              | 15–20                | 20–25              | 25–30              |
|--|-----------------|-----------------|--------------------|----------------------|--------------------|--------------------|
| Poisson’s ratio of saline–alkali soil  | 0.38            | 0.38            | 0.37               | 0.37                 | 0.37               | 0.36               |
| Shear modulus of saline–alkali soil/Pa   | $1 \times 10^6$ | $1 \times 10^6$ | $1.01 \times 10^6$ | $1.02 \times 10^6$   | $1.02 \times 10^6$ | $1.05 \times 10^6$ |
| Density of Saline–alkali Soil  | 1.653           | 1.682           | 1.725              | 1.746                | 1.775              | 1.793              |
| Coefficient of restitution between soil particles                                    | 0.42            | 0.39            | 0.38               | 0.36                 | 0.35               | 0.35               |
| The static friction coefficient between soil particles                               | 0.35            | 0.42            | 0.52               | 0.64                 | 0.78               | 0.96               |
| The dynamic friction coefficient between soil particles                              | 0.055           | 0.058           | 0.062              | 0.071                | 0.080              | 0.0885             |
| Poisson’s ratio of the fertilization pipe  |                 |                 |                    | 0.30                 |                    |                    |
| Shear modulus of the fertilization pipe/Pa   |                 |                 |                    | $7.9 \times 10^{10}$ |                    |                    |
| Density of the fertilization pipe/(kg/m <sup>3</sup> )                               |                 |                 |                    | 7860                 |                    |                    |
| Poisson’s ratio of fertilizer  |                 |                 |                    | 0.40                 |                    |                    |
| Shear modulus of fertilizer/Pa   |                 |                 |                    | $2.10 \times 10^7$   |                    |                    |
| Fertilizer density/(kg/m <sup>3</sup> )  |                 |                 |                    | $1.30 \times 10^3$   |                    |                    |
| Coefficient of restitution between fertilizers                                       |                 |                 |                    | 0.15                 |                    |                    |
| The coefficient of static friction between fertilizers                               |                 |                 |                    | 0.30                 |                    |                    |
| The coefficient of kinetic friction between fertilizers                              |                 |                 |                    | 0.25                 |                    |                    |
| Coefficient of restitution between fertilizer and fertilization pipe                 |                 |                 |                    | 0.36                 |                    |                    |
| The coefficient of static friction between the fertilizer and the fertilization pipe |                 |                 |                    | 0.25                 |                    |                    |
| Coefficient of kinetic friction between fertilizer and fertilization pipe            |                 |                 |                    | 0.20                 |                    |                    |
| Coefficient of restitution between soil and fertilizer                               | 0.35            | 0.35            | 0.33               | 0.33                 | 0.32               | 0.32               |
| The coefficient of static friction between soil and fertilizer                       | 0.23            | 0.26            | 0.27               | 0.28                 | 0.31               | 0.31               |
| The coefficient of kinetic friction between soil and fertilizer                      | 0.10            | 0.10            | 0.11               | 0.12                 | 0.12               | 0.12               |
| Coefficient of restitution between soil and fertilization pipe                       | 0.48            | 0.45            | 0.43               | 0.40                 | 0.38               | 0.35               |
| Coefficient of static friction between soil and fertilization pipe                   | 0.43            | 0.46            | 0.474              | 0.512                | 0.534              | 0.556              |
| Coefficient of kinetic friction between soil and the fertilization pipe              | 0.0454          | 0.0492          | 0.0528             | 0.0552               | 0.058              | 0.0608             |

Use EDEM 2020 (DEM Solutions Co., Ltd., Edinburgh, UK) to establish a soil tank model of saline–alkali soil after harrowing. The specific dimensions are 1500 mm in length, 800 mm in width, and 300 mm in height. A discrete element simulation model of the layered fertilization operation of the chisel-type depth-adjustable sub-soiling and fertilization device is shown in Figure 8.



**Figure 8.** Discrete element simulation model for layered fertilization operation. From top to bottom, different colors represent six different soil layers.

Establish a model of the chisel-type depth-adjustable sub-soiling and fertilizing device. According to the agronomic requirements for cotton sowing in the Yellow River Delta, set the forward speeds to be 3 km/h, 4 km/h, 5 km/h, 6 km/h, 7 km/h, 8 km/h, 9 km/h, and 10 km/h, respectively, with a fertilization rate of 435 kg/hm<sup>2</sup>. The discrete element simulation process of the layered fertilization operation is shown in Figure 9.

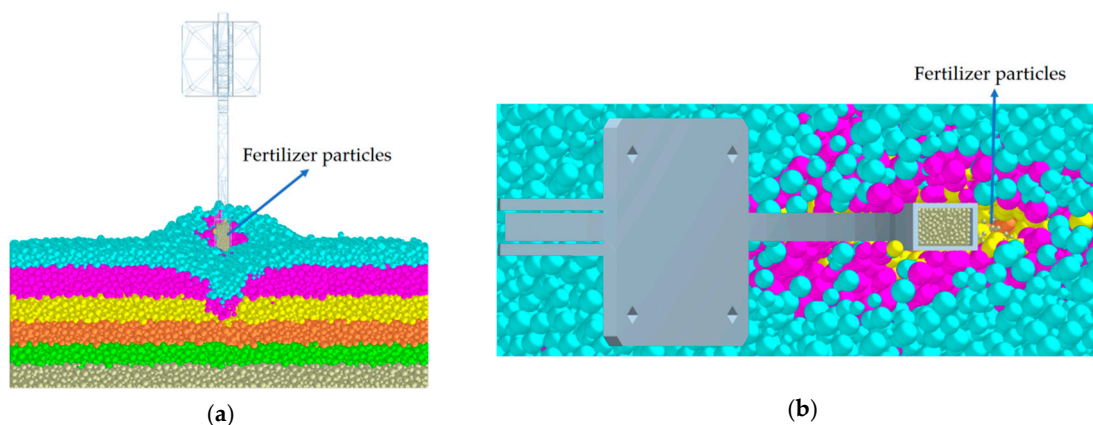


**Figure 9.** Discrete element simulation process of layered fertilization operation. (a) Simulation process of layered fertilization operation—rear view, (b) simulation process of layered fertilization operation—top view.

### 2.5.2. Influence of Forward Speed on the Effect of Variable-Rate Fertilization Operation

During the operation of the electronically controlled fertilizer discharging system, only the fertilization amount per unit area during operation needs to be input into the system, while the speed-measuring radar feeds in the forward speed of the entire machine. Based on these inputs, a mathematical model can be established by taking into account the relationships among parameters such as the forward speed of the entire machine, the fertilization amount per unit area, and the amount of fertilizer discharged in a single rotation of the fertilizer discharging device. This model is used to express the reasonable matching relationship between the forward speed and the rotational speed of the fertilization device. The mathematical model involving key parameters, such as the rotational speed of the fertilizer discharging device (that is, the rotational speed of the planetary gear reduction motor) and the forward speed, is presented as follows.

$$\begin{cases} \int S(t)dt = \int 10^{-3} \ln V(t)dt \\ \int FS(t)dt = \int M(t)dt \\ \int M(t)dt = \int 3.6fN(t)dt \end{cases} \quad (12)$$

In the formula, the symbols represent the following:

- $S(t)$ —The fertilized area at time  $t$ ; hm<sup>2</sup>;

- $l$ —Fertilization row spacing, cm;
- $n$ —The number of fertilizer distributors;
- $V(t)$ —The forward speed of the whole machine, km/h;
- $F$ —Fertilization amount per unit area, kg/hm<sup>2</sup>;
- $f$ —Fertilizer discharge amount per single rotation of the fertilizer applicator, g/r;
- $M(t)$ —The amount of fertilizer applied at time  $t$ , kg/hm<sup>2</sup>;
- $N(t)$ —The rotational speed of the fertilizer distributor (i.e., the rotational speed of the planetary gear reduction motor) at time  $t$ , r/min.

Through the mathematical model, the relationship between the forward speed of the whole machine and the rotational speed of the fertilizer discharging device can be calculated as follows:

$$V(t) = \frac{60fN(t)}{nFl} \quad (13)$$

It can be observed from the above formula that the relationship between the forward speed of the entire machine and the rotational speed of the fertilizer discharging device is associated with parameters such as the amount of fertilizer discharged per single rotation of the fertilizer discharging device, the number of fertilizer discharging devices, the amount of fertilizer applied per unit area, and the fertilization row spacing. Among them, according to the agronomic requirements for cotton planting, the amount of fertilizer applied per unit area is approximately 400 kg/hm<sup>2</sup>, the fertilization row spacing is 76 cm, and the number of fertilizer discharging devices is related to the structural design and performance of the entire machine. Therefore, the primary influencing factor of the relationship between the forward speed of the entire machine and the rotational speed of the fertilizer discharging device is the amount of fertilizer discharged per single rotation of the fertilizer discharging device.

The external fluted-wheel electronically controlled fertilizer discharging device is selected as the fertilization device. The electronically controlled fertilizer discharging device is the core component for realizing variable-rate fertilization. The main methods for it to achieve variable-rate fertilization are to change the rotational speed and the effective working width. The amount of fertilizer discharged per single rotation of the fertilizer discharging device is mainly related to the effective working width, and their basic relationship is

$$f = kL + c \quad (14)$$

In the formula, the symbols represent the following:

- $k$ —Proportional coefficient;
- $L$ —The effective working width of the electronically controlled fertilizer-discharging device, mm;
- $c$ —constant.

(1) Experimental research on the quantitative relationship between fertilizer discharge per single rotation and effective working width.

To measure the quantitative relationship between the amount of fertilizer discharged per single rotation of the selected external fluted-wheel electronically controlled fertilizer discharging device and its effective working width, a fertilization operation experiment was carried out.

① Experimental materials and instruments.

Controlled-release nitrogen fertilizer (with a particle size of about 2 mm), an electronic balance, a stopwatch, a seeder equipped with an external fluted-wheel electronically

controlled fertilizer discharging device, and a tractor equipped with an automatic driving system as the power source (which can ensure uniform forward movement).

② Experimental method.

Relevant tests on the external fluted-wheel electronically controlled fertilizer-discharging device were conducted in accordance with the *Technical Specification for Quality Evaluation of Fertilizer Machinery* NY/T1003-2006 [37].

The effective working widths of the external fluted-wheel electronically controlled fertilizer-discharging device were, respectively, set at 20 mm, 30 mm, and 40 mm. Subsequently, the rotational speeds were adjusted to 20, 25, 30, 35, and 40 r/min through the electric drive system. The amount of fertilizer discharged by the fertilizer-discharging device within one minute was measured. Fertilizer was collected using collection bags, and the weight of the fertilizer in the collection bags was measured with an electronic balance. Each data combination was tested three times, and after recording the data, the average value was calculated.

Numerical analysis of the quantitative relationship between the amount of fertilizer discharged per single rotation and the effective working width was completed to accurately calibrate the control parameters of the electric-driven fertilization system.

(2) Determination of the optimal parameter matching relationship between forward speed and rotational speed of the fertilizer discharging device.

According to the research conclusions presented in the previous text, when the forward speed rises to 4 km/h, there will be no intermixing among different layers during the layered fertilization process. When the speed reaches a range of 5–7 km/h, the layered fertilization effect is at its optimum. Therefore, a whole-machine speed within the range of 5–7 km/h is more suitable. Consequently, when the experimental forward speeds are set at 5 km/h, 5.5 km/h, 6 km/h, 6.5 km/h, and 7 km/h, the error between the set target fertilization amount and the actual fertilization amount is measured. By analyzing the error between the actual fertilization amount at each speed and the fertilization amount set by the system, the accuracy of the system is evaluated, and the optimal parameter-matching relationship between the forward speed and the rotational speed under different working widths is determined.

① Experimental materials and instruments.

Controlled release nitrogen fertilizer (with a particle size of about 2 mm), an electronic balance, a stopwatch, a seeder equipped with an external fluted-wheel electronically controlled fertilizer discharging device, and a tractor equipped with an automatic driving system as the power source (which can ensure uniform forward movement).

② Experimental site.

The Saline–Alkali Land Agricultural Experiment and Demonstration Base in the Yellow River Delta Agricultural High-tech Industry Demonstration Zone, Dongying City, Shandong Province.

③ Experimental method.

Relevant tests on the external fluted-wheel electronically controlled fertilizer-discharging device were carried out in accordance with the *Technical Specification for Quality Evaluation of Fertilizer Machinery* NY/T1003-2006 [37].

The seeder has 4 fertilizer discharging ports. The effective working widths for fertilizer discharge of the fertilizer discharging device are selected as 20 mm, 30 mm, and 40 mm. According to agronomic requirements, the target fertilization amount is set at 435 kg/hm<sup>2</sup>. The forward speeds of the tractor are set at 5 km/h, 5.5 km/h, 6 km/h, 6.5 km/h, and 7 km/h, respectively. The amount of fertilizer discharged by the fertilizer discharging device within a travel of 30 m is measured. Fertilizer is collected using collection bags, and the weight of the fertilizer in the collection bags is measured using an electronic balance

to calculate the actual fertilization amount. Each data combination is tested 3 times. After recording the data, the coefficient of variation and standard deviation of the consistency of the fertilizer discharging amount at each fertilizer discharging port are calculated. According to the requirements of the *Technical Specification for Quality Evaluation of Fertilizer Machinery NY/T1003-2006* [37], the coefficient of variation in the consistency of the fertilizer discharging amount at each fertilizer discharging port should be  $\leq 13\%$ .

$$q = \frac{\sum_{i=1}^n q_i}{n} \quad (15)$$

$$S = \sqrt{\frac{\sum_{i=1}^n (q_i - q)^2}{n - 1}} \quad (16)$$

$$CV = \frac{S}{q} \times 100\% \quad (17)$$

In the formula, the symbols represent the following:

- $q$ —The average of the average fertilizer-discharging amounts of each fertilizer-discharging port, g;
- $q_i$ —The average fertilizer-discharging amount of each fertilizer-discharging port, g;
- $S$ —The standard deviation of the consistency of the fertilizer-discharging amount of each fertilizer-discharging port, g;
- $CV$ —The coefficient of variation in the consistency of the fertilizer-discharging amount at each fertilizer-discharging port, %;
- $n$ —The number of fertilizer-discharging ports.

### 2.5.3. Field Test Verification

#### (1) Field test of fertilizer application rate deviation.

The optimal parameter combination test verification adopts the fertilizer application accuracy test method. The core evaluation parameter of fertilizer application accuracy is the fertilizer application rate deviation.

##### ① Experimental materials and instruments.

Controlled release nitrogen fertilizer (with a particle size of about 2 mm), an electronic balance, a stopwatch, a seeder equipped with an external fluted-wheel electronically controlled fertilizer discharging device, powered by a Dongfanghong 704 tractor (China Yituo Group Co., Ltd., Luoyang, China) equipped with an automatic driving system (which can ensure uniform forward movement), etc. As shown in Figure 10.



Figure 10. Field test equipment.

② Experimental site.

The Saline–Alkali Land Agricultural Experiment and Demonstration Base in the Yellow River Delta Agricultural High-tech Industry Demonstration Zone, Dongying City, Shandong Province.

③ Experimental method.

Relevant tests on the external fluted-wheel electronically controlled fertilizer-discharging device were carried out in accordance with the *Technical Specification for Quality Evaluation of Fertilizer Machinery* NY/T1003-2006 [37].

The effective working width for fertilizer discharge of the fertilizer discharging device is selected as 30 mm. According to agronomic requirements, the target fertilizer application rate is set at 435 kg/hm<sup>2</sup> and the working width of the seeder is 2.5 m. The amount of fertilizer discharged by the fertilizer discharging device within a travel of 30 m is measured. The fertilizer discharge amount is mainly obtained by measuring the weight difference in the fertilizer in the fertilizer tank before and after operation. Each data combination is tested 5 times. After recording the data, the fertilizer application rate deviation is calculated. According to the requirements of the *Technical Specification for Quality Evaluation of Fertilizer Machinery* NY/T1003-2006 [37], each fertilizer application rate deviation should be ≤15%.

$$\sigma_s = \frac{\left| \frac{10000(m_q - m_h)}{W} - M \right|}{M} \quad (18)$$

In the formula, the symbols represent the following:

- $\sigma_s$ —Fertilizer application rate deviation, %;
- $m_q$ —The mass of fertilizer in the fertilizer tank before operation, kg;
- $m_h$ —The mass of fertilizer in the fertilizer tank after operation, kg;
- $W$ —The area of fertilization operation, m<sup>2</sup>;
- $M$ —Target fertilization amount, kg/hm<sup>2</sup>.

Operation parameter determination: Set the operation parameters according to the optimized best combination of parameters after the simulation test for the field test.

(2) Field test of the effect of layered fertilization.

To verify the reliability of the discrete element simulation test and operation of the chisel-type variable-rate deep-layered fertilization device suitable for saline–alkali soil, a field test was carried out to verify the effect of layered fertilization.

① Experimental materials and instruments.

Controlled-release nitrogen fertilizer (with a particle size of about 2 mm), an excavating shovel, a meter stick, a seeder equipped with a chisel-type variable-rate deep-layered fertilization device powered by a Deutz-Fahr 1804 tractor equipped with an automatic driving system (which can ensure uniform forward movement), etc.

② Experimental site.

The Saline–Alkali Land Agricultural Experiment and Demonstration Base in the Yellow River Delta Agricultural High-tech Industry Demonstration Zone, Dongying City, Shandong Province.

③ Experimental method.

Determination of the coefficient of variation in fertilizer quantity uniformity in each soil layer: The seeder equipped with the chisel-type variable-rate deep-layered fertilization device is in operation. Since it is difficult to collect the distribution of fertilizer particles in the soil, the soil cross-section after the fertilization operation is taken in the test. Count the number of fertilizer particles in each layer and calculate the coefficient of variation in fertilizer quantity uniformity in each soil layer. Select an operation length of 10 m, dissect the soil every 1 m, complete 10 data statistics, and calculate the average value of the

coefficient of variation in fertilizer quantity uniformity in each soil layer. The calculation formula of the coefficient of variation in fertilizer quantity uniformity is

$$y_i = \sum_{i=1}^{10} \frac{\sqrt{\frac{1}{10-1}(x_i - \bar{x})^2}}{\bar{x}} \quad (19)$$

In the formula, the symbols represent the following:

- $y_i$ —Coefficient of variation in fertilizer quantity uniformity in each layer;
- $x_i$ —The number of fertilizer particles in the cross-section of each layer;
- $\bar{x}$ —The average number of fertilizer particles in the cross-section of each layer.

Determination of operation parameters: Set the operation parameters for the field experiment according to the optimal combination parameters optimized from the simulation experiment.

### 3. Results and Discussion

#### 3.1. Results of the Impact of Forward Speed on the Effect of Layered Fertilization Operation

The operation effects of the layered fertilization device under different forward speeds are shown in Figure 11. As can be seen from the figure, when the forward speed is relatively low, that is, the speed is less than or equal to 3 km/h, the fertilizer discharge amounts from the first and second fertilizer outlets are relatively large, while those from the third and fourth outlets are relatively small. A reasonable ratio of fertilizer application amounts in the upper and lower layers of deep fertilization cannot be achieved. At the same time, due to the low forward speed, the initial horizontal velocity of fertilizer particles is small, so the fertilizer particles fall rapidly before the soil is backfilled. The particles collide with each other, and when they collide with the backfilled soil again, the fertilizer particles cannot form an orderly layered fertilization effect. When the speed increases, the fertilizer discharge amounts from the first and second fertilizer outlets gradually decrease, while those from the third and fourth outlets relatively increase. When the speed increases to 4 km/h, there will be no mixed application phenomenon at the third and fourth outlets, but there will still be a large amount of fertilizer discharge at the first and second outlets, resulting in mixed application among layers. When the speed reaches 5–7 km/h, the fertilizer discharge amounts from each fertilizer outlet are relatively uniform, and the ratio of fertilizer application amounts in the upper and lower layers of deep fertilization is relatively reasonable. At the same time, within this speed range, the soil backfilling rate and the fertilizer movement rate are relatively well matched. The backfilled soil buries the fertilizers in each layer, respectively, and the layered fertilization effect reaches the best. When the speed exceeds 7 km/h, although the fertilizer discharge amounts from each fertilizer outlet can still meet the agronomic requirements, due to the relatively fast forward speed, the initial horizontal velocity of the fertilizer is too large, resulting in a large displacement. A large number of collisions occur with the already backfilled soil, and the phenomenon of mixed application among layers begins to appear, resulting in a poor fertilization effect. When the speed reaches 10 km/h, the forward speed of the fertilization shovel is too fast, causing a large displacement in the soil. When the soil movement displacement is large, the backfilling time increases, resulting in the soil not being backfilled in time, causing mixed application of fertilizers in each layer and reducing the layered fertilization operation effect of the fertilization device.

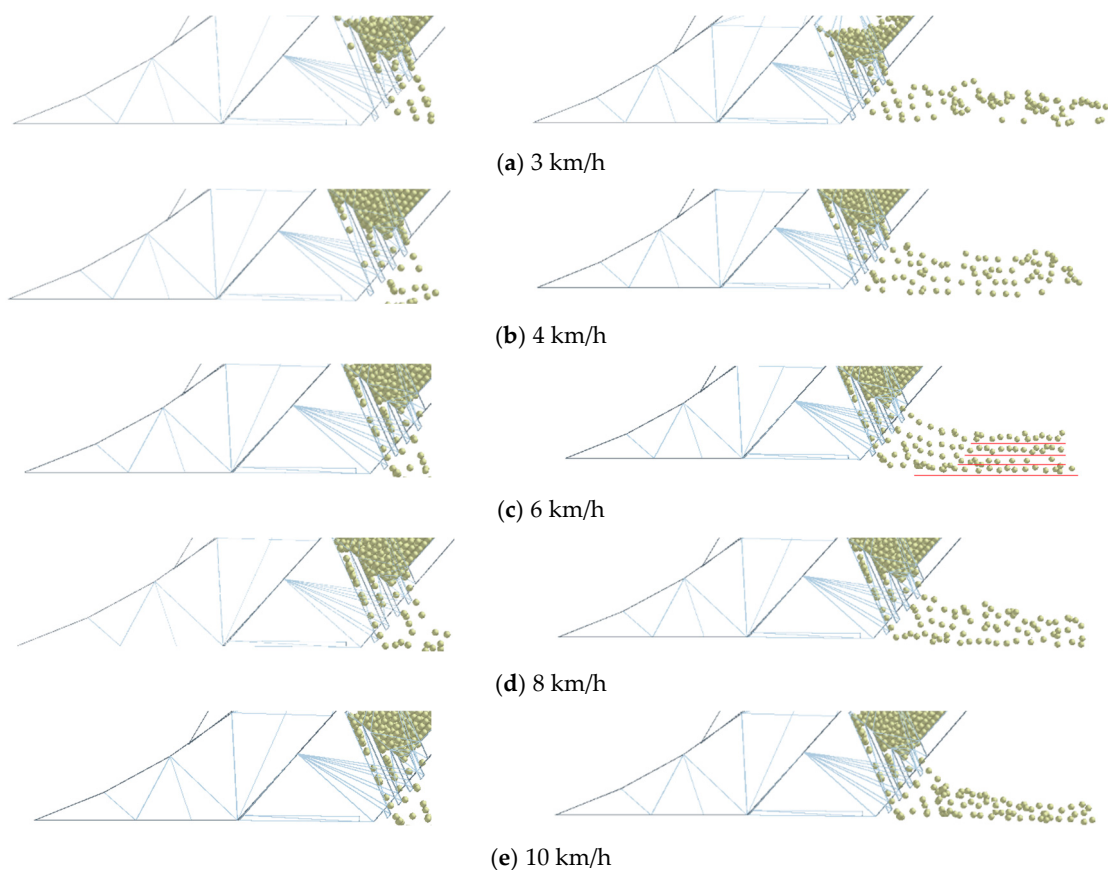


**Figure 11.** The operational effects of the layered fertilization device at different forward speeds using the DEM.

3.2. Results of the Impact of Forward Speed on the Effect of Variable-Rate Fertilization Operation

(1) Test results of the quantitative relationship between fertilizer discharge per single rotation and effective working width.

According to the above-mentioned test methods, the tests were carried out and the data were recorded, as shown in Table 6.

**Table 6.** Test Results of fertilizer discharge per single rotation.

| Number | Effective Working Width/mm | Rotational Speed/(r/min) | 1min Fertilizer Discharge Amount/g | Fertilizer Application Amount per Revolution/g |
|--------|----------------------------|--------------------------|------------------------------------|--|
| 1      | 20                         | 20                       | 716.40                             | 35.82  |
| 2      | 20                         | 25                       | 903.75                             | 37.15  |
| 3      | 20                         | 30                       | 1082.70                            | 37.47  |
| 4      | 20                         | 35                       | 1268.75                            | 37.45  |
| 5      | 20                         | 40                       | 1452.80                            | 37.51  |
| 6      | 30                         | 20                       | 1052.00                            | 52.60  |
| 7      | 30                         | 25                       | 1333.75                            | 53.85  |
| 8      | 30                         | 30                       | 1599.30                            | 54.51  |
| 9      | 30                         | 35                       | 1869.00                            | 54.62  |
| 10     | 30                         | 40                       | 2147.20                            | 54.58  |
| 11     | 40                         | 20                       | 1266.00                            | 63.30  |
| 12     | 40                         | 25                       | 1632.00                            | 65.28  |
| 13     | 40                         | 30                       | 1962.60                            | 66.42  |
| 14     | 40                         | 35                       | 2288.65                            | 66.39  |
| 15     | 40                         | 40                       | 2620.80                            | 66.52  |

Based on the recorded and calculated data, a scatter plot with smooth lines of the rotational speed and the fertilizer discharge amount per single rotation under different effective working widths was drawn, as shown in Figure 12. It can be seen from the figure that when the rotational speed is lower than 30 r/min, the stability of the fertilizer discharge amount per single rotation of the electric-driven fertilizer discharging system is poor. However, when the rotational speed is higher than 30 r/min, the fertilizer discharge amount per single rotation tends to be stable, and the coefficient of variation in the fertilizer discharge amount is small.

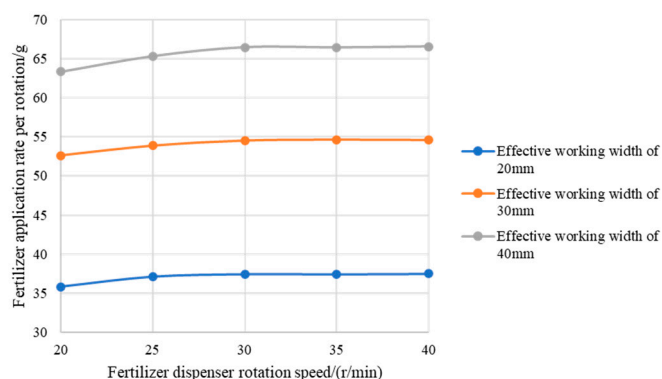


**Figure 12.** Relationship between the rotational speed of the fertilizer discharging device and the fertilizer discharge amount per single rotation.

Within the range of rotational speeds with a small coefficient of variation in the fertilizer discharge amount, the average fertilizer discharge amounts per single rotation for effective working widths of 20 mm, 30 mm, and 40 mm are calculated to be 37.48 g, 54.57 g, and 66.44 g, respectively. Then, a linear fitting analysis is conducted on the relationship between the fertilizer discharge amount per single rotation and the rotational speed of the fertilizer discharging device, as shown in Figure 13.

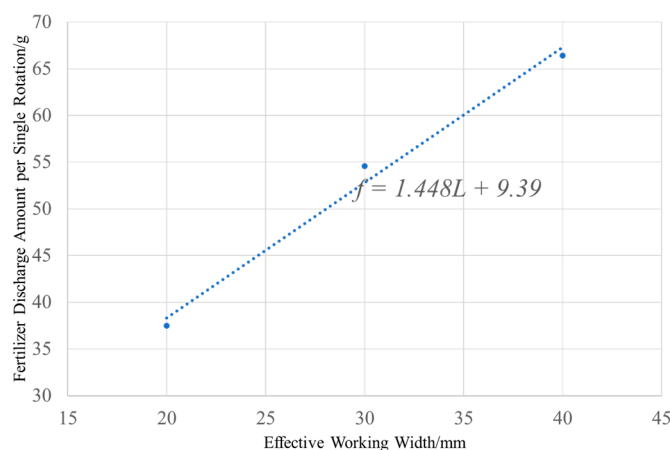


**Figure 13.** Relationship between the effective working width of the fertilizer discharging device and the fertilizer discharge amount per single rotation.

Through linear-fitting analysis, the quantitative relationship between the fertilizer-discharge amount per single rotation of the fertilizer discharging device and the effective working width is mainly as follows.

After calculation and verification, its linear-fitting coefficient is above 0.95, which can be used to match the forward speed of the machine with the rotational speed of the fertilizer discharging device to achieve precise fertilization.

(2) Measurement results of the optimal parameter matching relationship between forward speed and rotational speed of the fertilizer discharging device.

Fertilization uniformity test: According to the above-mentioned test methods, the tests were carried out and the data were recorded, as shown in Table 7.

**Table 7.** Fertilizer discharge amount results of the fertilizer discharging device at different rotational speeds and forward speeds.

| Number | Forward Speed/(km/h) | Effective Working Width/mm | Coefficient of Variation in Fertilizer Application Rate/% |
|--------|----------------------|----------------------------|---|
| 1      | 5                    | 20                         | 1.68  |
| 2      | 5                    | 30                         | 1.36  |
| 3      | 5                    | 40                         | 1.12  |
| 4      | 5.5                  | 20                         | 1.38  |
| 5      | 5.5                  | 30                         | 1.13  |
| 6      | 5.5                  | 40                         | 0.89  |
| 7      | 6                    | 20                         | 0.78  |
| 8      | 6                    | 30                         | 0.61  |
| 9      | 6                    | 40                         | 0.64  |
| 10     | 6.5                  | 20                         | 1.48  |
| 11     | 6.5                  | 30                         | 1.25  |
| 12     | 6.5                  | 40                         | 0.96  |
| 13     | 7                    | 20                         | 2.04  |
| 14     | 7                    | 30                         | 1.92  |
| 15     | 7                    | 40                         | 1.06  |

When the target fertilizer application rate is fixed, the rotational speed of the fertilizer discharging device at different forward speeds can be obtained from the relationship formula between the forward speed of the whole machine and the rotational speed of the fertilizer discharging device (Equation (13)) and the relationship formula between the fertilizer discharge amount per single rotation and the effective working width (Equation (14)). Combined with the above table, it can be seen that, although the coefficient of variation in the fertilizer discharge amount is  $\leq 13\%$  under the matching of various parameters, when the forward speed is 5.5–6.5 km/h, the coefficient of variation in the fertilizer discharge amount is less than 1.5%, especially for some combined test results, which are less than 1%. At the same time, when comparing different effective working widths, the combination of a forward speed of 6 km/h and a width of 30 mm has the lowest coefficient of variation and is the best. Through calculation, it is obtained that when the forward speed is 5.5–6.5 km/h, the optimal matching rotational speed is 36–38.5 r/min; when the forward speed is 6 km/h and the width is 30 mm, the rotational speed is about 36.5 r/min.

### 3.3. Results of Field Test Verification

(1) Results of field test of fertilizer application rate deviation.

According to the results of the impact of forward speed on the effect of the variable-rate fertilization operation, the forward speeds are set at 5.5 km/h, 6 km/h, and 6.5 km/h, respectively. According to the field test method of fertilizer application rate deviation, the tests are carried out and the data are recorded, as shown in Table 8.

As can be seen from the above table, after setting the target fertilizer application rate, the deviation in the fertilizer application rate varies at different forward speeds. The main reason is that the change in the forward speed leads to a change in the rotational speed of the fertilizer discharging device, and the stability of the fertilizer discharge amount varies under different rotational speeds of the fertilizer discharging device. When the forward speed increases, the rotational speed of the fertilizer discharging device rises. Since the effective working width of the fertilizer discharge port is fixed, the rate of fertilizer discharge

by gravity decreases, resulting in an increase in the deviation of the fertilizer application rate. When the forward speed decreases, the rotational speed of the fertilizer discharging device decreases, leading to a reduction in the stability of the fertilizer discharging device and an increase in the deviation of the fertilizer application rate. According to the results of the test verification data, the fertilization effect is optimal when the forward speed is around 6 km/h.

**Table 8.** Deviation between target fertilizer application rate and actual fertilizer application rate.

| Number | Forward Speed/(km/h) | Deviation in Fertilizer Application Amount/% |      |      |      |      | Average Value of Fertilizer Application Amount Deviation/% |
|--------|----------------------|--|------|------|------|------|--|
|        |                      | 1  | 2    | 3    | 4    | 5    |  |
| 1      | 5.5                  | 4.63   | 5.37 | 6.05 | 5.83 | 6.32 | 5.64   |
| 2      | 6.0                  | 2.65   | 3.28 | 2.09 | 2.76 | 3.03 | 2.76   |
| 3      | 6.5                  | 7.13   | 6.85 | 5.32 | 6.28 | 6.35 | 6.39   |

## (2) Results of the field test of the layered fertilization effect.

Set the operation parameters according to the optimized best combination of parameters from the simulation test to conduct the field test of the layered fertilization effect. Set the forward speeds to 5.5 km/h, 6 km/h, and 6.5 km/h, respectively. According to the field test method for the coefficient of variation in fertilizer quantity uniformity in each soil layer, carry out the tests and record the data. The field test equipment and results are shown in Figure 14.



**Figure 14.** Field Test Equipment and Results (a) Field test equipment; (b) Results of field tests.

After calculation, the measurement results of the coefficient of variation in fertilizer quantity uniformity in each soil layer are shown in Table 9 and Figure 15.

**Table 9.** Measurement results of the coefficient of variation in fertilizer quantity uniformity in each soil layer.

| Number | Forward Speed/(km/h) | Average Value of the Coefficient of Variation in Fertilizer Quantity Uniformity in Each Soil Layer/% |      |      |      |
|--------|----------------------|--|------|------|------|
|        |                      | 1  | 2    | 3    | 4    |
| 1      | 5.5                  | 9.83   | 7.56 | 7.36 | 6.85 |
| 2      | 6.0                  | 7.62   | 6.32 | 6.06 | 5.65 |
| 3      | 6.5                  | 8.79   | 7.31 | 6.93 | 6.43 |

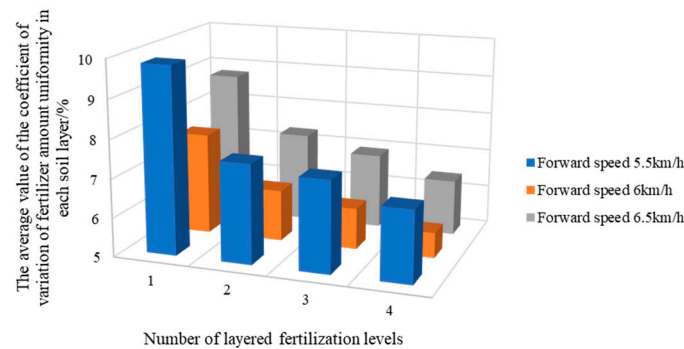


**Figure 15.** Measurement results of the coefficient of variation in fertilizer quantity uniformity in each soil layer.

After setting the target fertilizer application rate, the coefficient of variation in fertilizer quantity uniformity in each soil layer varies at different forward speeds. The main reason is that changes in the forward speed lead to alterations in soil disturbance and backfilling conditions. The measurement results of the coefficient of variation in fertilizer quantity uniformity in each soil layer show that when the speed is between 5.5 km/h and 6.5 km/h, the coefficient of variation in fertilizer quantity uniformity in each soil layer is less than 10%, which can meet the requirements of precise fertilization. However, when the speed is 6 km/h, the coefficient of variation in fertilizer quantity uniformity in each soil layer is the smallest. At the same time, compared to the simulation test, in the simulation test, when the speed reaches 5–7 km/h, the fertilizer quantity at each fertilizer outlet is relatively uniform. Therefore, according to the experimental verification data, the fertilization effect is the best when the forward speed is about 6 km/h.

#### 4. Conclusions

This paper devises a chisel-type variable hierarchical deep fertilization device suitable for saline–alkali soil. The research findings are as follows:

(1) Emphasis was laid on the design of the shovel-tip structure based on dynamics and the enhancement of its performance. The penetration angle was determined to be  $20^\circ$  and the clearance angle for soil entry was  $10^\circ$ . Design research was conducted on the energy-saving and drag-reducing structure of the shovel shank, and the shank curve was determined for the design of the shovel shank. The design of the fertilization pipe structure was accomplished. The angle between the fertilization baffle and the fertilization pipe wall was  $115^\circ$ , the angle between the fertilization pipe and the horizontal plane was  $50^\circ$ , and the lengths of the baffles at different fertilization openings were 16 mm, 27 mm, 50 mm, and 65 mm, respectively.

(2) Taking cotton production as an example, in accordance with the fertilization agronomic requirements of cotton cultivation, an electronically controlled fertilizer discharging device was designed. The device employs a traditional external fluted-wheel fertilizer discharger, along with an STM32F103RCT6 embedded micro-controller and a 36GX555 planetary reduction motor. The rest mainly consists of an NCE80H11-type MOS-tube-based motor driver, a speed-measuring radar based on the Doppler principle, an STM32 single-chip micro-computer, and other system hardware components.

(3) Research was carried out on the impact of forward speed on the operational effects of layered and variable-rate fertilization. Through field experiments, it was determined that the optimal fertilization effect is achieved when the forward speed is 6 km/h. The average deviation of the fertilization amount is 2.76%, and the average values of the coefficient of variation in fertilizer amount uniformity in each soil layer are 7.62%, 6.32%, 6.06%, and

5.65%. The experimental results meet the predefined goals and comply with the design requirements.

**Author Contributions:** Conceptualization, N.X. and X.L.; methodology, N.X.; software, N.X.; validation, N.X., Z.X., J.Y., Z.G., Y.T., C.X. and D.W.; resources, X.L. and D.W.; data curation, N.X.; writing—original draft preparation, N.X.; writing—review and editing, X.L.; project administration, X.L. All authors have read and agreed to the published version of the manuscript.

**Funding:** This research was supported by National Key R&D Program of China (2022YFD2300101) and Key Research and Development Program of Shandong Province (Science and Technology Demonstration Project) (2024SFGC0405) and Shandong Provincial Cotton Industry Technology System Innovation Team Machinery Post Expert Project (SDAIT-03-09) and Key R&D Program (Major Science and Technology Innovation Project) in Shandong Province (2021CXGC010813) and Project of Mechanization of Sowing and Field Management Post in the National Peanut Industry Technology System (CARS-13).

**Institutional Review Board Statement:** Not applicable.

**Data Availability Statement:** The original contributions presented in the study are included in the article, further inquiries can be directed to the corresponding authors.

**Conflicts of Interest:** The authors declare no conflicts of interest.

## References

- Office of the Leading Group of the Third National Land Survey of the State Council, Ministry of Natural Resources, National Bureau of Statistics. *Bulletin on the Main Data of the Third National Land Survey*; 2021 Office of the Leading Group of the Third National Land Survey of the State Council, Ministry of Natural Resources, National Bureau of Statistics: Beijing, China, 2021.
- Guo, K.; Feng, X.H.; Wu, J.W.; Chen, X.B.; Ju, Z.Q.; Sun, H.Y.; Liu, X.J. Research Progress on Mechanism and Technology of Integrated Regulating on Soil Water, Salt and Fertility under Fertile Plough Layers Construction in Saline-Alkali Soils. *Acta Pedol. Sin.* **2024**, *61*, 29–381–9.
- Shen, T.O. Effects of Deep Ploughing and Straw Returning to Improve Saline-Alkali Land on Soil Characteristics of Saline-Alkali Land. Master's Thesis, Neimenggu Agricultural University, Hohhot, China, 2022.
- Ding, X.L.; Cui, D.Y.; Liu, T.; Wang, S.; Zhao, L.X. Optimization design and experiment of precision variable fertilizer device. *J. Chin. Agric. Mech.* **2019**, *40*, 5–12.
- Liu, X.D. Design and Experiment on Precise Discharge-Apply Fertilizer System of Rapeseed Planter. Ph.D. Dissertation, Huazhong Agricultural University, Wuhan, China, 2022.
- Liu, X.D.; Wang, X.P.; Chen, L.Y. Design and experiments of layered and quantitative fertilization device for rapeseed seeder. *Trans. Chin. Soc. Agric. Eng.* **2021**, *37*, 1–10.
- Wang, B.T.; Bai, L.; Ding, S.P.; Yao, Y.X.; Huang, Y.X.; Zhu, R.X. Simulation and experimental study on impact of fluted-rollerfertilizer key parameters on fertilizer amount. *J. Chin. Agric. Mech.* **2017**, *38*, 1–6.
- Wang, J.F.; Gao, G.B.; Weng, W.X.; Wang, J.W.; Yan, D.W.; Chen, B.W. Design and Experiment of Key Components of Side Deep Fertilization Device for Paddy Field. *Trans. Chin. Soc. Agric. Mach.* **2018**, *49*, 93–104.
- Wang, Y.X.; Liang, Z.J.; Cui, T.; Zhang, D.X.; Qu, Z.; Yang, L. Design and Experiment of Layered Fertilization Device for Corn. *Trans. Chin. Soc. Agric. Mach.* **2016**, *47*, 163–169.
- Zhang, J.X.; Liu, H.M.; Gao, J.; Lin, Z.H.; Chen, Y. Simulation and Test of Corn Layer Alignment Position Hole Fertilization Seeder Based on SPH. *Trans. Chin. Soc. Agric. Mach.* **2018**, *49*, 67–72.
- Zhu, Q.Z.; Wu, G.W.; An, X.F.; Chen, L.P.; Meng, Z.J.; Zhao, C.J. Relationship model of fertilizer outlet location and fertilizer application depth of depth-fixed application device of base-fertilizer. *Trans. Chin. Soc. Agric. Eng.* **2018**, *34*, 8–17.
- Zhu, Q.Z.; Wu, G.W.; Chen, L.P.; Meng, Z.J.; Shi, J.T.; Zhao, C.J. Design of stratified and depth-fixed application device of base-fertilizer for winter wheat based on soil-covering rotary tillage. *Trans. Chin. Soc. Agric. Eng.* **2018**, *34*, 18–26.
- Shi, Y.Y.; Chen, M.; Wang, X.C.; Odhiambo, M.; Zhang, Y.N.; Ding, W.M. Analysis and Experiment of Fertilizing Performance for Precision Fertilizer Applicator in Rice and Wheat Fields. *Trans. Chin. Soc. Agric. Mach.* **2017**, *48*, 98–103.
- Shi, J.S.; Qi, H.K.; Sun, F.C.; Zhao, J.G.; Zhao, X.S.; Ma, Z.K.; Li, J.C.; Hao, J.J.; Ma, Y.J. Optimization design and experiment of subsoiling and anti-blocking layered fertilizer shovel. *J. Hebei Agric. Univ.* **2020**, *43*, 96–102.
- Song, S.L.; Zhang, D.C.; Tang, Z.H.; Zheng, X.; Chen, X.G.; Yang, H.J.; Meng, X.J. Parameter optimization and test of layered fertilization boot based on discrete element method. *J. China Agric. Univ.* **2020**, *25*, 125–136.

16. Xiao, W.L.; Xiao, W.F.; Liao, Y.T.; Zhang, Q.S.; Wei, G.L.; Liao, Q.X. Design and performance test of plough-type positive deep fertilization device for rapeseed direct planter. *J. Huazhong Agric. Univ.* **2018**, *37*, 131–137.
17. Dun, G.Q.; Yu, C.L.; Guo, Y.L.; Ji, W.Y.; Islamk, K.R.; Du, J.X. Design and Experiment of Double-gear Type Fertilizer Apparatus. *Trans. Chin. Soc. Agric. Mach.* **2020**, *51*, 88–96.
18. Sugirbay, A.M.; Zhao, J.; Nukeshev, S.O.; Chen, J. Determination of pin-roller parameters and evaluation of the uniformity of granular fertilizer application metering devices in precision farming. *Comput. Electron. AGR* **2020**, *179*, 105835. [[CrossRef](#)]
19. May, S.; Kocabiyik, H. Design and development of an electronic drive and control system for microgranular fertilizer metering unit. *Comput. Electron. AGR* **2019**, *162*, 921–930. [[CrossRef](#)]
20. Bangura, K.; Gong, H.; Deng, R.L.; Tao, M.; Liu, C.; Cai, Y.H. Simulation analysis of fertilizer discharge process using the Discrete Element Method (DEM). *PLoS ONE* **2020**, *15*, e0235872. [[CrossRef](#)]
21. Li, P.L.; Mustafa, U.; Sang-Heon, L.; Chris, S. A new method to analyse the soil movement during tillage operations using a novel digital image processing algorithm. *Comput. Electron. AGR* **2019**, *156*, 43–50. [[CrossRef](#)]
22. Barr, J.B.; Desbiolles, J.; Ucgul, M.; Fielke, J.M. Bentleg furrow opener performance analysis using the discrete element method. *Biosyst. Eng.* **2020**, *189*, 99–115. [[CrossRef](#)]
23. Barr, J.B.; Ucgul, M.; Desbiolles, J.M.A.; Fielke, J.M. Simulating the effect of rake angle on narrow opener performance with the discrete element method. *Biosyst. Eng.* **2018**, *171*, 1–15. [[CrossRef](#)]
24. Wang, B. Design and Experiment of Components for Rotary Tillage and Deep Fertilization of Rapeseed Direct Seeding Machine. Master's Thesis, Huazhong Agricultural University, Wuhan, China, 2022.
25. Liu, W.H. Design and Simulation Study of Corn Ridge Double-Row Strip Tillage Fertilizer Machine. Master's Thesis, Northeast Forestry University, Harbin, China, 2023.
26. Liao, Y.T.; Gao, L.P.; Liao, Q.X.; Zang, Q.S.; Liu, L.C.; Fu, Y.K. Design and Test of Side Deep Fertilizing Device of Combined Precision Rapeseed Seeder. *J. AGR Match-Iran.* **2020**, *51*, 65–75.
27. Yang, Q.L.; Huang, X.Y.; Wang, Q.J.; Li, H.W.; Wang, Y.B.; Wang, L.Y. Structure Optimization and Experiment of Corn Layered Fertilization Device. *J. AGR Match-Iran.* **2020**, *51*, 175–185.
28. Han, L.J.; Yu, J.J.; Jin, J.J.; Xie, D.S.; Zhang, J.Z.; Zhang, R.H. Design and experiment of electronic control fertilization device for tubeless wheat seeder. *J. Chin. Agric. Mech.* **2021**, *42*, 27–34.
29. Zhao, Y.Z.; Wang, Y.; Gong, Z.P.; Yang, Y.Q.; Zhao, S.H.; Gou, J.B. Design and Experiment on Side Deep and Layered Fertilizing and Seeding Components of No-tillage Planter. *J. AGR Match-Iran.* **2021**, *52*, 41–50.
30. Ma, C. Design and Experiment of Deep Fertilization Strip Tillage Device for Corn in Northeast China. Master's Thesis, Chinese Academy of Agricultural Mechanization Sciences, Beijing, China, 2022.
31. Song, J.L. Design and Experiment of Corn No-Tillage Planter Stubble Subsoiling Layered Fertilization Seedbed Preparation Device. Master's Thesis, Anhui Agricultural University, Hefei, China, 2023.
32. Dun, G.Q.; Chen, H.T.; Feng, Y.N.; Yang, J.L.; Li, A.; Zha, Z.H. Parameter optimization and test of key parts of fertilizer allocation device based on EDEM software. *Trans. Chin. Soc. Agric. Eng.* **2016**, *32*, 36–42.
33. Liu, L.J.; Ma, C.; Liu, Z.J. EDEM-based Parameter Optimization and Experiment of Full-layer Fertilization Shovel for Strip Subsoiling. *Trans. Chin. Soc. Agric. Mach.* **2021**, *52*, 75–83.
34. Ding, S.P. Simulation and Test of the Fertilizer Adjusting Ratio and Layered Fertilization Based on Discrete Element Method. Master's Thesis, Northwest A&F University, Xianyang, China, 2018.
35. Xu, N.; Xin, Z.X.; Yuan, J.; Gao, Z.H.; Tian, Y.; Xia, C.; Liu, X.M.; Wang, D.W. Calibration of Discrete Element Simulation Parameters and Model Construction for the Interaction Between Coastal Saline Alkali Soil and Soil-Engaging Components. *Agriculture* **2025**, *15*, 7. [[CrossRef](#)]
36. Du, X.; Liu, C.L.; Jiang, M.; Yuan, H.; Dai, L.; Li, F.L.; Gao, Z.P. Design and Experiments of a Layered Fertilizer Shovel for Maize. *INMATEH-Agric. Eng.* **2022**, *68*, 305–314. [[CrossRef](#)]
37. NY/T1003-2006; Technical Specification for Quality Evaluation of Fertilizer Machinery. Ministry of Agriculture of the People's Republic of China: Beijing, China, 2006.

**Disclaimer/Publisher's Note:** The statements, opinions and data contained in all publications are solely those of the individual author(s) and contributor(s) and not of MDPI and/or the editor(s). MDPI and/or the editor(s) disclaim responsibility for any injury to people or property resulting from any ideas, methods, instructions or products referred to in the content.